so that σ^{AI} becomes comparable to σ^{DI} at relatively low energies. The estimated cross sections are plotted in Fig. 2. It shows the dominance of σ^{AI} for the incident kinetic energy of approximately 12 keV and higher, $pa_0 \gtrsim 30$. The energy parameters used in the evaluation of (3) and (5) are generated by the single-particle model[5]; $\Delta_{3s} = 96.5$ Ry and $\Delta_{3p} = 92.1$ Ry for the DI, and $\Delta_{2s} = 180\ \text{Ry} = \Delta_{2p}$ for the AI excitations. From the extrapolation fit of α discussed earlier, one obtains $\alpha_L = 0.90$, as compared with $\alpha_L(Z_r = 0) = 0.97$. The AI contribution comes mainly from the $2p$ excitation followed by the Auger emission, while the $2s$ excitation contributes about 4% to the total AI. The contribution of the $3s$ electrons to the AI by excitations to states just below the ionization threshold is also estimated to be about 3% and less. For the DI cross section, the $3p$ ionization dominates over the $3s$ electrons by approximately 5 to 1.

In summary, I have shown that, for reactions involving highly stripped ions, σ^{DI} alone can often lead to a gross underestimate of the impact ionization cross section. The relative magnitude of M_C (outer shell) and M_D (inner shell) is important, but not sufficient to make the AI process dominant, and the branching ratio α_i plays an important role which warrants much further study. As Z_C increases, we expect that the dominance of the AI process will be more prevalent even at fairly low Z_r.

The calculation presented here is only approximate and requires more extensive studies, but its qualitative conclusions are not expected to be seriously affected by the details, which will be reported elsewhere.[9]

[a]Work supported in part by the U. S. Energy Research and Development Administration under Contract No. E11-1-2276.

[1]Y. Hahn and K. M. Watson, Phys. Rev. A 7, 491 (1973).
[2]Y. Hahn, Phys. Rev. A (to be published).
[3]H. A. Bethe and R. W. Jackiw, *Intermediate Quantum Mechanics* (Benjamin, New York, 1968).
[4]Y. Hahn and K. M. Watson, Phys. Rev. A 6, 548 (1972); Y. Hahn, Phys. Rev. A 13, 1326 (1976).
[5]P. P. Szydlik and A. E. S. Green, Phys. Rev. A 9, 1885 (1974).
[6]W. Bambynek *et al.*, Rev. Mod. Phys. 44, 716 (1972).
[7]M. H. Chen and B. Crasemann, Phys. Rev. A 12, 959 (1975).
[8]C. P. Bhalla, Phys. Rev. A 12, 122 (1975), and J. Phys. B 8, 2792 (1975).
[9]Y. Hahn, to be published.
[10]U. Fano and M. Inokuti, ANL Report No. ANL-76-80, 1976 (unpublished).

Steady-State Model of a Flat Laser-Driven Target

F. S. Felber
Naval Research Laboratory, Washington, D. C. 20375
(Received 16 February 1977)

A steady-state model of a plasma slab, accelerated by interaction with laser radiation, determines temperature, velocity, and density profiles and boundaries consistent with laser intensity and wavelength and slab mass and acceleration. Density-profile modification is caused by laser pressure. Plasma flows subsonically into the critical surface, and supersonically out.

In an earlier Letter[1] exact transmission coefficients were calculated for intense light incident on a plasma slab in which ions were frozen. In this paper a steady-state model of a plasma slab, accelerated by its interaction with laser radiation, is treated by one-dimensional (1D) steady-flow hydrodynamic equations in an accelerated frame of reference. The cold unablated fluid, the ablation layer, both classical and flux-limited hot conduction regions, the critical surface, and the underdense blowoff are all considered. A global description determines the temperature, density, velocity, and boundaries as well. Approximate analytic solutions are given in each of the plasma regions.

The ablation layer, containing a steep density gradient separating cold dense fluid from hot low-density plasma, moves at the front of the thermal wave and is accelerated by the rocket reaction to the ablation. Nevertheless Boris has demonstrated through time-dependent numerical simulations that the temperature profile at the ablation layer is steady in an accelerated reference frame, and provided a simplified analytic model of the steady temperature profile at the ablation layer.[2]

The quasi-steady-state model presented here accounts self-consistently for the (slow) increase in acceleration of the slab as a result of the diminishing mass of cold fluid being accelerated. While a slab geometry reveals most of the important physics, and will be used in forthcoming papers to consider flat-target experiments and instability at the ablation layer, the model readily transforms to a spherical geometry. Max, McKee, and Mead[3] have found analytic steady-state solutions for plasma flow in the hot conduction region of spherical laser targets, and Gitomer, Morse, and Newberger[4] have treated spherical flow with an artificial mass source.

The model is formulated in terms of time-independent solutions of the continuity, momentum, and energy equations,

$$0=\frac{\partial\rho}{\partial t}=-\frac{\partial}{\partial x}(\rho v),$$
$$0=\frac{\partial}{\partial t}(\rho v)=-\frac{\partial}{\partial x}(\rho v^2+P)+\rho g-\left(\frac{I_a+2I_r}{c}\right)\delta(x-x_c), \qquad (1)$$
$$0=\frac{\partial\mathcal{E}}{\partial t}=-\frac{\partial}{\partial x}(Pv+\mathcal{E}v+q)+\rho g v+I_a\,\delta(x-x_c).$$

Here v is the velocity of a volume element of mass density ρ, temperature (in energy units) T, pressure $P=\rho T/m_i$, ion mass m_i, and local energy density $\mathcal{E}=\frac{1}{2}(3P+\rho v^2)$; I_a (I_r) is the absorbed (reflected) laser flux. The laser energy and momentum are regarded as deposited at the critical surface $x=x_c$. The momentum-deposition term causes gradient steepening and density shelves at the critical surface that have been observed experimentally,[5] and calculated theoretically[6] by other means. The effective gravity g must be included in the energy equation as the product of force density ρg with velocity v. It cannot be omitted, as by Brueckner, Jorna, and Janda.[7] The heat flux q at any point in the hot conduction region is considered to be the lesser in magnitude of the classical flux $q_{\rm class}=-KT^{5/2}T'$ and limited flux $q_{\rm lim}=l\rho(T/m_i)^{3/2}T'|T'|^{-1}$. A prime denotes d/dx, $KT^{5/2}$ is the conductivity, and the flux-limit parameter l lies in the author-dependent range[3] $0.5\lesssim l\lesssim 60$. An upper bound, $l\lesssim 3$, for this model is derived below.

The continuity equation implies constant momentum density $\rho v=\rho_0 v_0$. Fluid quantities evaluated at the origin, chosen at the surface of maximum density, are denoted by a subscript zero. Then the momentum and integrated energy equations in the overdense fluid simplify to two first-order equations in ρ and T,

$$\rho'=\rho(T'-m_i g)[m_i v_0^2(\rho_0/\rho)^2-T]^{-1},$$
$$q=(T,T',\rho)=-\tfrac{1}{2}(\rho_0 v_0/m_i)[5(T-T_0)+m_i v_0^2(\rho_0^2/\rho^2-1)-2m_i g x]-KT_0^{5/2}m_i g, \qquad (2)$$

that can be solved by a Runge-Kutta code in classical-conduction and flux-limited regions. Solutions near the ablation layer are shown in Fig. 1. The flux $\sim T^{5/2}T'$ in the cold fluid rises monotonically towards the heat source, but the temperature gradient T', while positive definite, is not necessarily monotonic. At maximum density, $T_0'=m_i g$; conduction is enhanced by increased acceleration.

If the dimensionless gravity $\Gamma\equiv(m_i^2KT_0^{3/2}/\rho_0 v_0)g$ and Mach number $M\equiv(m_i v^2/T)^{1/2}$ are both $\ll 1$ in the cold fluid, then approximate analytic solutions of (2) are

$$T\approx T_0(1-\tfrac{8}{25}\Gamma+2m_i g x/5T_0),\quad \rho\approx\rho_0(1+3m_i g x/5T_0),\quad (-T_0/m_i g\lesssim x\lesssim 0). \qquad (3)$$

Indeed the laminar ablation rate is generally much less than the local sound speed at the ablation layer in ablative implosions, though not in exploding-pusher targets. A sonic point ($M=1$) can occur in the cold fluid at

$$x_s=-\frac{T_0}{m_i g}\left[\frac{5+M_0^2}{2}+\Gamma\left(\frac{M_0\rho_0}{\rho(x_s)}\right)^5-\Gamma-3\left(\frac{M_0\rho_0}{\rho(x_s)}\right)^2\right].$$

If $M\ll 1$ and $\Gamma\ll 1$, then an approximate analytic solution of (2) in the hot classically conducting region, valid for $0\lesssim x\lesssim T_0/m_i g$, is

$$x(T)\approx\frac{4m_i KT_0^{5/2}}{25\rho_0 v_0}[(\tau^{5/2}-1)+\tfrac{5}{3}(\tau^{3/2}-1)+5(\tau^{1/2}-1)], \qquad (4)$$

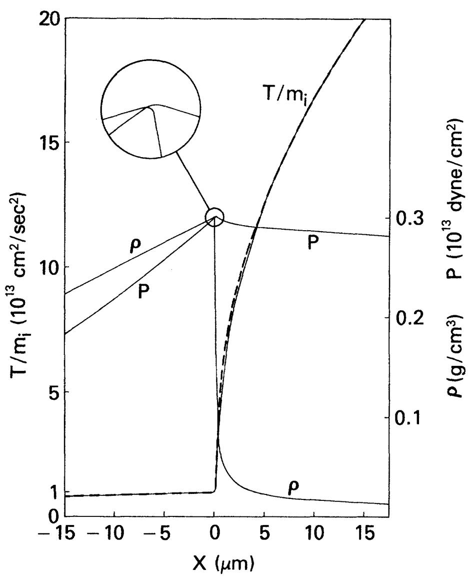

FIG. 1. Temperature, density, and pressure profiles at the ablation layer calculated from the model with $T_0/m_i = 10^{13}$ cm^2/sec^2, $v_0 = 2.2\times10^5$ cm/sec, $\rho_0 = 0.3$ g/cm^3, and acceleration $g = 3\times10^{15}$ cm/sec^2. Dashed curve, analytic temperature approximation [Eqs. (3)–(4)].

in which $\tau \equiv T/T_0$. The analytic solutions (3) and (4) for cold and hot conduction regions are compared in Fig. 1 with the numerical solution of (2). At high temperatures (4) can be inverted:

$$T \approx (25\rho_0 v_0/4m_i K)^{2/5} x^{2/5} - \tfrac{2}{3}T_0, \quad T \gg T_0.$$

At sufficiently high temperature and low density, the heat flux may saturate in the overdense region. The solutions of (2) for both classical flux and saturated flux are matched where $q_{\rm class} = q_{\rm lim}$. In a saturated-flux region, (2) implies[8]

$$(5 + M^2 - 2l/M)T = 2m_i gx + (5 - 2\Gamma + M_0^2)\,T_0 \approx 2m_i gx + 5T_0. \quad (5)$$

The gravity gives the Mach number a spatial dependence and boost; the flow is assisted, and onset of flux limiting delayed.

At the critical surface, conservation of mass requires $\rho_+ v_+ = \rho_- v_-$, so that the jumps in density and velocity are related by

$$v_+ \Delta\rho = -\rho_- \Delta v. \quad (6)$$

The notation concerning the jump in any variable u is defined by $\Delta u \equiv u_+ - u_- \equiv u(x_c + 0) - u(x_c - 0)$. All energy deposited at the critical surface is assumed to be conducted into the much more massive and colder overdense region, so that $q = 0$ in the underdense region, and an adiabatic equation of state applies there. Then with $\Delta T = 0$ and $T(x_c) \equiv T_c$, $\Delta q = -q(\rho_-, T_c) > 0$. The jump conditions from (1) are

$$\Delta\rho = -m_i(I_a + 2I_r)/(T_c - m_i v_-^2\varphi)c,$$
$$\Delta v = (\varphi - 1)v_-, \quad (7)$$

where $\varphi \equiv [1 + 2(I_a - \Delta q)/\rho_- v_-^3]^{1/2}$. The case is considered for which the heat conducted away from x_c does not exceed the laser energy deposited there, so that $\varphi > 1$. Together (6) and (7) imply

$$I_a + 2I_r = (\rho_- c/m_i)(T_c - m_i v_-^2\varphi)(1 - 1/\varphi). \quad (8)$$

Since $I_a + 2I_r > 0$ and $\varphi > 1$, then $m_i v_-^2 < T_c$. Thus steady flow into the critical surface is subsonic in the rest frame of the critical surface.[9] Then (5) implies that the flux-limit parameter l must be less than 3 for a flux-limited region to exist in steady state. This upper bound is comparable with recent experimental values and theoretical predictions.[3,10]

Mass, momentum, and energy conservation across the critical surface insufficiently constrain the solution.[6] A reasonable added constraint derived in Ref. 6 for a related problem, and independent of ponderomotive force, is $\rho_- = \frac{1}{2}\rho_c[M_-^2 - \ln(M_-^2) - 1](1 - M_-)^{-2}$. The density shelves and subsonic flow into the critical surface are features of other theoretical treatments[6] as well, and are seen here to be caused exclusively by laser momentum deposition. Ordinarily a ponderomotive-force term proportional to $\rho d|E|^2/dx$ is appended to the momentum equation to model the effects of the electric field E in the underdense region, imposing spatially periodic fluctuations on density and velocity profiles. In this model the momentum equation is averaged over many wavelengths to iron out the effects of the ponderomotive force, $\langle \rho d|E|^2/dx\rangle_x = 0$, and leave only the gross profiles of the steady flow of an ideal, adiabatic gas in the underdense region.

The exact solutions of (1) for the underdense, adiabatic gas are

$$v^2 - 5(T_c/m_i)[1 - (v_+/v)^{2/3}] = v_+^2 + 2g(x - x_c),$$
$$\rho = \rho_+ v_+/v, \quad T = T_c(v_+/v)^{2/3}. \quad (9)$$

On physical grounds T must decrease away from the heat source at x_c. Then (9) implies that the flow out of the critical surface must be supersonic, $m_i v_+^2 > \frac{5}{3}T_c$. The gravity determines the boundaries self-consistently. Let the total plasma mass per area, m, be specified. Since momentum density is uniform, during a time δt a thin layer of mass $\delta m = \rho_L v_L \delta t = \rho_- v_- \delta t$ is effec-

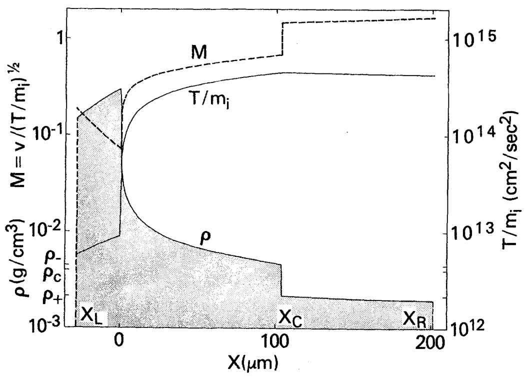

FIG. 2. Density, temperature, and Mach-number profiles of global slab model. Specified were the absorbed flux $I_a = 10.2$ TW/cm^2, reflected flux $I_r = 10.2$ TW/cm^2, total mass $m = 0.733$ mg/cm^2, acceleration $g = 3\times 10^{15}$ cm/sec^2, critical density $\rho_c = 4\times 10^{-3}$ g/cm^3, and critical temperature $T_c/m_i = 4.50\times 10^{14}$ cm^2/sec^2; the coefficient of conductivity was $K = 10^{-33} m_i^{-7/2}$ (cgs). Self-consistency of the global model required a critical surface at x_c, left and right boundaries at x_L and x_R, and upper and lower shelf densities ρ_- and ρ_+ as shown. No saturation of heat flux occurs here for the flux-limit parameter $l > 1.79$.

tively transferred from the left boundary x_L to the right boundary x_R at higher velocity v_R. The change in momentum, $\delta p = \delta m(v_R - v_L)$, must be compensated by an acceleration of the whole plasma to the left, since the hydrodynamic forces are internal, causing an effective gravity

$$g = \rho_- v_- (v_R - v_L)/m. \qquad (10)$$

This condition determines the approximate slab boundaries, and completes the global description of the laser-plasma interaction. Figure 2 shows the self-consistent profiles and boundaries found by specifying I_a, I_r, m, g, ρ_c, and T_c only.

Since the jump conditions are not satisfied at the slab boundaries, the steady-state assumption breaks down near the boundaries. Equation (10) is good, however, as long as the widths of the unsteady slab ends are much less than the overall width of the slab. The gravity increases,

$$dg/dt = \rho_- v_- (dv_R^2/dx - dv_L^2/dx)/2m,$$

and can only be considered steady during an interval Δt if

$$\Delta t \ll 2(v_R - v_L)/(dv_R^2/dx - dv_L^2/dx). \qquad (11)$$

If the cold fluid is no wider than about $T_0/m_i g$, and the underdense region is wider than about $T_c/m_i g$, then (3), (9), and (11) imply a characteristic time scale for growth of the acceleration of v_R/g. The dynamical development of a slab can be followed over longer time periods by respecifying gravity and intensity if desired, and repeating the integration of (2).

I wish to thank J. P. Boris for valuable comments and suggestions on this topic, and S. E. Bodner and D. L. Book for advice and encouragement. This work was supported by a National Research Council Resident Research Associateship at the Naval Research Laboratory.

[1]F. S. Felber and J. H. Marburger, Phys. Rev. Lett. 36, 1176 (1976).

[2]J. P. Boris, Comments on Plasma Physics and Controlled Fusion, to be published; Naval Research Laboratory Memorandum Report No. 3427 (1977), and Bull. Am. Phys. Soc. 21, 1103 (1976).

[3]C. E. Max, C. F. McKee, and W. C. Mead, University of California Report No. UCRL-78458 (1976).

[4]S. J. Gitomer, R. L. Morse, and B. S. Newberger, Phys. Fluids 20, 234 (1977).

[5]H. C. Kim, R. Stenzel, and A. Y. Wong, Phys. Rev. Lett. 33, 886 (1974).

[6]R. E. Kidder, in *Proceedings of Japan-U. S. Seminar on Laser Interaction with Matter*, edited by C. Yamanaka (Tokyo International Book Co., Tokyo, 1975); K. Lee *et al.*, Phys. Fluids 20, 51 (1977).

[7]K. A. Brueckner, S. Jorna, and R. Janda, Phys. Fluids 17, 1554 (1974).

[8]A similar equation was first derived in Ref. 3 for spherical geometry, $T_0 = 0$ and $g = 0$.

[9]This result, implied by consideration of laser momentum deposition, agrees with Ref. 6 and with K. A. Brueckner and R. S. Janda, to be published, and is contrary to Ref. 4, in which laser momentum deposition was not treated.

[10]F. C. Young *et al.*, Appl. Phys. Lett. 30, 45 (1977); W. M. Manheimer, D. G. Colombant, and B. H. Ripin, Phys. Rev. Lett. 38, 1135 (1977).